



Shahrood University of
Technology



Iranian Society of
Mining Engineering
(IRSM)

Investigating Effect of Tunnel Size, Rock Mass Conditions, and In-Situ Stresses on Stability of Tunnels

Hafeezur Rehman^{1,2}, Ahmad Shah¹, Mohd Hazizan Bin Mohd Hashim^{2*}, Naseer Muhammad Khan¹, Wahid Ali¹, Kausar Sultan Shah³, Muhammad Junaid³, Rafi Ullah^{4,5}, and Muhammad Bilal Adeel⁶

1. Department of Mining Engineering, Faculty of Engineering, Balochistan University of Information Technology, Engineering and Management Sciences (BUITEMS), Quetta, Pakistan

2. School of Materials and Mineral Resources Engineering, University Sains Malaysia, Engineering Campus, Nibong Tebal Penang, Malaysia

3. Department of Mining Engineering, Karakoram International University, Gilgit-Baltistan, Pakistan

4. Department of Geotechnics and Transportation, Faculty of Civil Engineering, Universiti Teknologi Malaysia, Johor Bahru, Johor, Malaysia

5. Department of Geological Engineering, Faculty of Engineering, Balochistan University of Information Technology, Engineering and Management Sciences (BUITEMS), Quetta, Pakistan

6. Department of Transportation and Geotechnical Engineering, National University of Science and Technology, Risalpur Campus, Pakistan

Article Info

Received 24 September 2022

Received in Revised form 12
October 2022

Accepted 9 November 2022

Published online 9 November
2022

DOI: [10.22044/jme.2022.12294.2231](https://doi.org/10.22044/jme.2022.12294.2231)

Keywords

Critical strain

Stress reduction factor

Capacity diagram

Tunnel shape and size

In-situ stresses

Abstract

The major factors affecting tunnel stability include the ground conditions, in-situ stresses, and project-related features. In this research work, critical strain, stress reduction factor (SRF), and capacity diagrams are used for tunnel stability analysis. For this purpose, eighteen tunnel sections are modelled using the FLAC2D software. The rock mass properties for the modelling are obtained using the RocLab software. The results obtained show that tunnel deformations in most cases are within the safety limit. Meanwhile, it is observed that the rock mass quality, tunnel size, and in-situ stresses contribute to the deformation. The resulting deformations also affect SRF. SRF depends on the in-situ stresses, rock mass quality, and excavation sequence. The capacity diagrams show that the liner experience stress-induced failures due to stress concentration at the tunnel corners. This study concludes that tunnel stability analysis must include an integrated approach that considers the rock quality, in-situ stress, excavation dimensions, and deformations.

1. Introduction

Stable and economic excavation of underground structures is the primary concern during the design stage. For this purpose, various methods and tools are used during design and construction. For choosing an excavation method, the effects of size, shape, and in-situ stress level are considered. The excavation method and the factors mentioned above are mutually responsible for the ground behaviour [4]. Based on the ground response, different instability issues can occur. For tunnel stability analysis, strain-based [4] and stress-based [2], approaches are often used. These techniques help predict instability, excavation sequence, and support requirements [4, 1]. In short, the

excavation scheme and tunnel support requirements are primarily responsible for the construction schedule, cost, and safety [9, 4].

Stress-induced instability is critical for tunnel construction and operation, not only during the design and construction stage but also in the service life [9, 4]. In deep tunnels, the excavation-induced tangential stresses (σ_θ) are high and the radial stresses (σ_r) are negligible near the tunnel periphery, which result in tunnel failure. The variation of σ_θ and σ_r from the tunnel periphery is shown in Figure 1 [9]. σ_r was gradually increased from zero with the distance from the tunnel boundary. On the other hand, σ_θ was at its peak at the periphery, and

✉ Corresponding author: mohd_hazizan@usm.my (M. Hazizan Bin Mohd Hashim).

gradually decreased with the distance. In the case of brittle rock, the stress-induced failure appears in the form of rockburst, and can pose unsafe conditions [10, 4, 3]. In the case of soft rock, it results in squeezing [11]. The overstressed support in such situations also causes support failure. Heavy and deformable rock support may be required in such stress-dominant failure cases [5, 1].

In rock engineering design, analytical, empirical, numerical, observational, and the combined system approach are used. For tunnel stability analysis, the empirical techniques combined with numerical modelling are easy and economical at the design stage of the project. Also these techniques have received international acceptance, and can be adopted at any stage of the project.

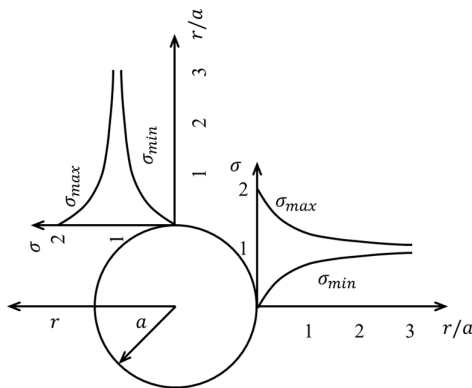


Figure 1. Variation in principal stresses around an underground excavation.

Currently, several tunnel stability evaluation techniques like critical strain [4], stress variable [1], capacity diagram [5], and stress reduction factor (SRF) [2] are used along with numerical modelling. However, the researchers and field experts use an individual approach for a particular case study. From a review of the relevant literature, techniques that incorporate all the parameters in tunnel stability analysis are apparently less discussed. Therefore, this work attempts to conduct tunnel stability analysis by incorporating all the essential parameters. For this purpose, two tunnel projects, named Lawari road and Kohala hydropower projects, from Pakistan were numerically modelled based on their intact rock and rock mass data. For modelling, FLAC^{2D}, an explicit two-dimensional finite-difference program, was used. This work is the continuation and extension of the previous research work and the numerical model used in the paper for the comparison of the two excavation sequences has been validated already. The numerical modelling results, along with the tunnel size, applied support, and intact rock strength were

used for the stability evaluation. The capacity diagram, critical strain, and stress reduction factor approaches were the evaluation standards used in this work.

2. Tunnel Stability Evaluation Techniques

During tunnel design and construction, stress or strain is determined at the tunnel periphery. Therefore, tunnel stability assessment is often carried out using stress or strain-based techniques. Sometimes, the installed supports are sufficiently enough to stabilize the tunnel; however, the support reaches a critical situation under loading. In the following sections, stress-based, strain-based, and shotcrete stability evaluation techniques are discussed.

2.1. Critical strain for tunnel deformation

Tunnel convergence is the strain-based instability issue that arises during the excavation stage. To evaluate these issues, Sakuri [4] has extended the definition of critical strain to tunnelling, and diagrammatically correlated the rock mass strength and the strain in the rock mass surrounding the tunnel. This strain is the ratio of tunnel deformation to the tunnel radius. The strain measurement is practical and easier than stress-based evaluation, as the latter needs constitutive equations for interpretations [2]. The practical applications of this evaluating technique were further extended by Hoek, considering the amount of support required to limit the tunnel deformation to a specified level. Keeping in mind this deformation concept, Hoek and Marinos [11] have proposed a diagram for the squeezing level prediction by relating the percentage ratio of tunnel deformation to their diameter with the rock mass strength to in-situ stress ratio. The British Tunnelling Society also adopts the critical evaluation technique as a guideline during the design and construction of the tunnel. Referring to the limitations and expanding the scope of the critical strain, the Sakuri assessment diagram for the tunnel stability evaluation was modified, and more factors were included along with the rock mass strength including RMR, Q-value, and rock mass deformation modulus [2, 3]. Different studies used the critical strain approach for stability evaluation during tunnelling [6, 5, 3].

2.2. SRF for brittle failure

During the Q-system development for the tunnel support design, an empirical table was suggested for the brittle failure in hard rock, which was

modified later . The table was for the SRF characterization in the Q-system for the rock mass quality determination. SRF is based on the ratio between intact rock strength (σ_c) and major principal stress (σ_1) or excavation induced tangential stress (σ_θ), as shown in Table 1.

Although the purpose of Table 1 was the characterization of SRF and determination of the

rock mass quality quantitatively, however, when the σ_θ values are known, then it is possible to evaluate the brittle type of failure around the tunnel. This approach was used as an empirical rock bursting evaluation technique in the recently completed complex Neelum Jhelum Hydro Electric Power Project (NJHEPP).

Table 1. Relationship of stress level with SRF based on strength-stress ratios .

	Stress level	σ_c/σ_1	σ_θ/σ_c	SRF
1	Low stress near surface, open joints	> 200	< 0.01	2.5
2	Medium stress, favorable stress condition	200-10	0.01-0.3	1
3	High stress, very tight structure. Typically, favorable to stability, and may be unfavorable to wall stability	10-5	0.3–0.4	0.5–2
4	Moderate slabbing after > 1 h in massive rock	5-3	0.5–0.65	5–50
5	Slabbing and rock burst after a few minutes in massive rock	3-2	0.65–1.0	50–200
6	Heavy rock burst (strain-burst) and immediate dynamic deformation in massive rock	< 2	> 1.0	200–400

2.3. Capacity diagram for the shotcrete stability

The thrust–bending moment and thrust—shear force interaction diagrams were developed for shotcrete/ liner stability evaluation [5]. This diagrammatical/graphical evaluation approach is the function of thrust force (N), bending moment (M), and shear force (Q) on the shotcrete. The N and M relation for failure in tension and compression is defined in Equations 1 and 2, respectively.

$$N = \frac{|M|At}{2I} + \frac{\sigma_t A}{FS} \tag{1}$$

$$N = -\frac{|M|At}{2I} + \frac{\sigma_c A}{FS} \tag{2}$$

where A, I, t, FS, σ_t , and σ_c are the area, moment of inertia, thickness, factor of safety (FOS), tensile, and compressive strength of shotcrete, respectively. For a particular value of FS, M_{cr} (critical value of bending moment) is defined for tensile and compressive failures in Equation 3.

$$M_{cr} = \pm \frac{I}{t} \times \frac{\sigma_c - \sigma_t}{FS} \tag{3}$$

The diagram based on Equations 1-3 is the thrust bending moment diagram.

Similarly, the relationship between N and Q for failure in tension and compression is shown in Equations 4 and 5, respectively.

$$N = \frac{\sigma_c \cdot A}{FS} - \frac{9}{4} \times \frac{Q^2 FS}{\sigma_c A} \tag{4}$$

$$N = \frac{\sigma_t \cdot A}{FS} - \frac{9}{4} \times \frac{Q^2 FS}{\sigma_t A} \tag{5}$$

For a specific FS value, Q_{cr} (critical value of shear force) is defined for tensile and compressive in Equation 6.

$$Q_{cr} = \pm \frac{A}{FS} \sqrt{-\frac{4}{9} \sigma_c \sigma_t} \tag{6}$$

The diagram based on Equations 4-6 is the thrust shear force diagram.

3. Project Description, Geology of Area, and Rock Mass Properties

3.1. Lowari tunnel project

The 8.5 km Lowari tunnel (LT) is the longest road tunnel in the northern part of Pakistan (Figure 2), and has been available for public transportation since 2017. During the construction period, a major design modification switched the Lowari Rail Tunnel (LRT) to a road tunnel named Modified Road Tunnel (MRT). The 7.12 m span LRT, designed with the concept of piggyback rail, was modified to an 11.17 m span two-way road tunnel.

The LT project is located in a seismically active zone, where the Indian plate subducts the Eurasian Continental plate . The geological investigations were physically verified during the construction of

LRT and MRT. Five geological units were exposed along the tunnel longitudinal axis including the biotite granite unit, the granite unit, the meta sediment unit, the metavolcanic unit, and the meta igneous unit [12]. The properties of two dominant rock units, named granodiorite and gneiss, are used in this research work. The intact rock properties are

shown in Table 2. Due to the rough topography along the tunnel axis, three vertical stress conditions, 10, 15, and 20 MPa, were used in the modelling. A total of 12 cases were modelled in the study for the LT (6 for LRT and 6 for MRT) project, considering the tunnel size, stress conditions, and rock units.

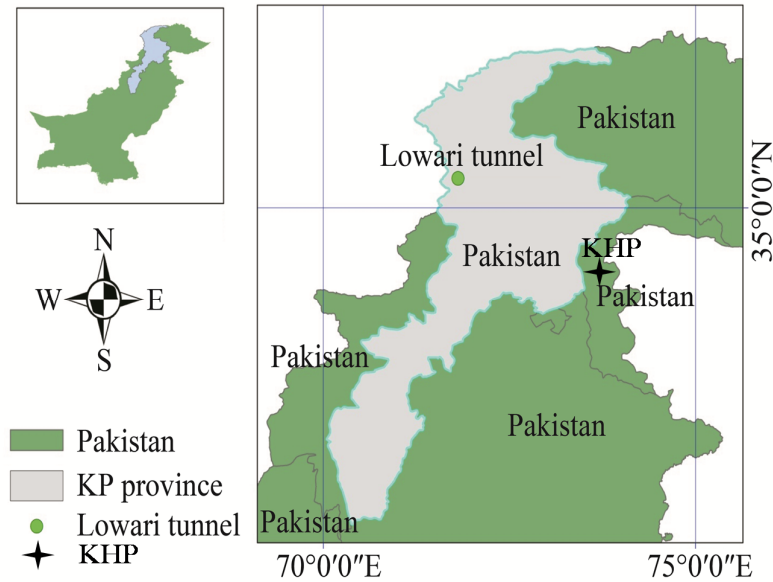


Figure 2. Location of projects.

3.2. Kohala Hydro Power (KHP) project

The 17.5 km super-long headrace tunnel is the major component of 1100 MW of KHP on the Jhelum river, located in the Azad Jammu and Kashmir (AJ & K), the north-eastern area of Pakistan (Figure 2) [6]. This project area is seismically active, and belongs to the western part of the Himalayas. The headrace tunnels are planned through a stratigraphic sequence of alternative beds of sandstone (SS), siltstone, and mudstone of the Murree formation. The project is nearby the recently completed NJHEP project, and therefore, has a similar setting [4]. SS is a dominant rock in the area, which is further divided into SS1 and SS2 based on their properties. The intact rock properties are shown in Table 2. The vertical stresses at the designed tunnel elevation reach 26 MPa in the project [6]; however, for comparison and limiting the modelling number, similar stress

values were taken in this study like the LT project. Taking the rock mass conditions, in-situ stresses, and tunnel size (8.5 m horse-shoe shape), six cases are modelled for the headrace tunnel of KHP.

Roclab software is used to extrapolate the Table 2 data to rock mass. The programming of this simple software is based on the generalized Hoek–Brown failure criteria to determine the input parameters for numerical modelling. In rock mass, the number of fractures along with their characteristics have a dominant role in the mechanical properties and rock mass behavior [6, 4, 1, 5, 2]. The calculated strength parameters of rock mass are shown in Table 3. The table reveals that the mechanical properties in descending order are for gneiss, granodiorite, SS1, and SS2 rock masses. The table also indicates that with depth, the rock mass cohesion values increase, while their internal friction values decrease.

Table 2. Intact rock mechanical and physical properties along with rock mass properties.

Case No.	Project	Rock type	Vertical stresses, MPa	UCS, MPa	m_i	GSI	Unit weight, kN/m ³	E, GPa
01	LRT	Granodiorite	10	75	29	65	27.20	31.9
02			15					
03			20					
04		Gneiss	10	100	23	64	26.98	52.5
05			15					
06			20					
07	MRT	Granodiorite	10	75	29	65	27.20	31.9
08			15					
09			20					
10		Gneiss	10	100	23	64	26.98	52.5
11			15					
12			20					
13	KHP	SS1	10	80	17	60	27.67	27.0
14			15					
15			20					
16		SS2	10	50	17	50	26.86	27.0
17			15					
18			20					

Table 3. Rock mass properties for numerical modelling.

Case No.	m_b	s	a	c, MPa	ϕ , °	E, GPa	σ_t , MPa	σ_{cm} , MPa
01	8.309	0.021	0.502	2.62	54.73	20.13	0.185	10.65
02				3.29	52.02			
03				3.92	49.94			
04	6.358	0.018	0.502	2.82	54.66	32.02	0.288	13.42
05				3.51	51.90			
06				4.14	49.84			
07	8.309	0.021	0.502	2.62	54.73	20.13	0.185	10.65
08				3.29	52.02			
09				3.92	49.94			
10	6.358	0.018	0.502	2.82	54.66	32.02	0.288	13.42
11				3.51	51.90			
12				4.14	49.84			
13	4.074	0.012	0.503	2.19	49.96	14.04	0.231	8.56
14				2.73	46.99			
15				3.22	44.83			
16	2.851	0.004	0.506	1.50	43.50	8.29	0.068	3.01
17				1.93	40.32			
18				2.31	38.04			

4. Tunnel Excavation and Support

In LRT and MRT project, NATM (New Austrian Tunnelling Method) method, also known as the observational method, was used. This observational method discusses the procedures during the design and construction of tunnel excavation, and summarizes the procedures of tunnel excavation and support design. The actual tunnel support, applied in LRT and MRT, was adopted in this study. The LRT excavation is full face; however, the widely used top heading and bench excavation approach was adopted in MRT.

The actual sequence was a special case due to the major design modification of the project.

In KHPP, the top heading and bench excavation sequence is used for the tunnel excavation and support. The empirical suggested support based on a modified tunnel quality system (Q-system) was adopted. The widely used Q-system for tunnel support design reveals that rock bolt spacing varies with the quality of rock mass and their length, considering the tunnel's size [2, 4]. In the case of shotcrete, the international acceptable empirical systems believe that the thickness of shotcrete

depends on the quality of rock mass and tunnel size [8].

The details of shotcrete and rock bolts are given in Table 4. The table shows that NATM considers thick shotcrete and fewer rock bolts than the empirical systems. The higher reliability on shotcrete termed the NATM a shotcrete method [FHWA-NHI-10-034]. By comparing the LRT cases (1-6) with MRT (7-12), the installed support is the same although the span of the MRT is larger

than the LRT. This trend is due to twice releasing stresses in the actual excavation sequences of the LRT followed by MRT in the LT project. In empirical suggested support cases (13-18), shotcrete thickness is in the range 06-09 cm (taking highly stressed jointed rock mass environment), and therefore, 09 cm thick shotcrete is selected from the safety point of view. The rock bolt spacing ranges from 1.7-1.8, resulting in 13 rock bolts in the tunnel periphery (crown and walls).

Table 4. Applied tunnel support in numerical modelling.

Excavation method	Case No.	Rock bolt length, m	Nos of rock bolts	Shotcrete thickness, cm
NATM	1-6	4	7	15
NATM	7-12	4	7	15
Empirical	13-18	3	13	09

5. Numerical modelling

For tunnel analysis, FLAC version 7.0 is used in this work. FLAC is an explicit 2D finite-difference program appropriate for modelling sequential excavation. The full face excavation (a single excavation stage) is only implemented for LRT (cases 1-6), and was followed by support installation of Table 4. In MRT and KHP, tunnels were excavated using two excavation stages, top heading, and bench excavation approach. After the top heading, supports were applied in the crown, followed by bench excavation, and then support application in the tunnel walls. Generally, each excavation stage consists of three construction steps:

1. Initial excavation (through nul model)
2. Spraying of soft shotcrete (using liner option of the structure element) and installation of rock bolt support
3. Shotcrete hardening via changing the mechanical properties of the shotcrete

The FLAC model region, showing full face and top heading and bench excavation, for the three tunnel sizes are shown in Figure 3.

For simulation, the model boundary was far enough to eliminate their effect on the results. Around the tunnel boundary, the mesh was comparatively fine enough for precise results. The model boundaries were fixed, except the top. The vertical boundaries were fixed for horizontal movement, and the bottom was fixed for vertical movement. For analysis, the modified Hoek-Brown model, which is based on the non-linear relation between major and minor principal (σ_1 and σ_3) stresses, was used. In the models, the rock mass parameters, defined in Table 3, were used as the

input. The vertical stresses (σ_{yy}) were due to gravity and applied stresses command at the top of the model. A FISH function was used for the complete in-situ stress conditions in the model. In the construction steps, 40%, 30%, and 30% relaxation were used for excavation, applying soft shotcrete and rock bolt, and hard shotcrete, respectively. The Table 4 support pattern was adopted as per the excavation and support sequence.

6. Results and discussion

The FLAC models are solved statically for the complete excavation sequence of LRT and top heading and bench excavation of the MRT and KHP projects. The results in terms of displacement and tangential stresses around the tunnel periphery were obtained. Further, the axial forces, shear forces, and bending moments in shotcrete were also obtained from the modelling for stability evaluation.

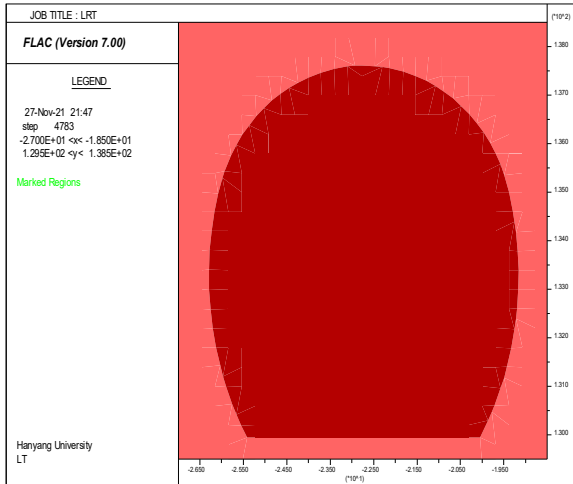
6.1. Evaluation based on critical strain

The critical strains were determined for all cases, considering the maximum displacements from FLAC modelling and tunnel size. The total displacements were calculated after solving the model statically. For this purpose, the grid point (GP) displacement option was used. The critical strain, as defined in section 2.1, and rock mass strength value for each case were plotted for strain-based tunnel stability evaluation, as shown in Figure 4.

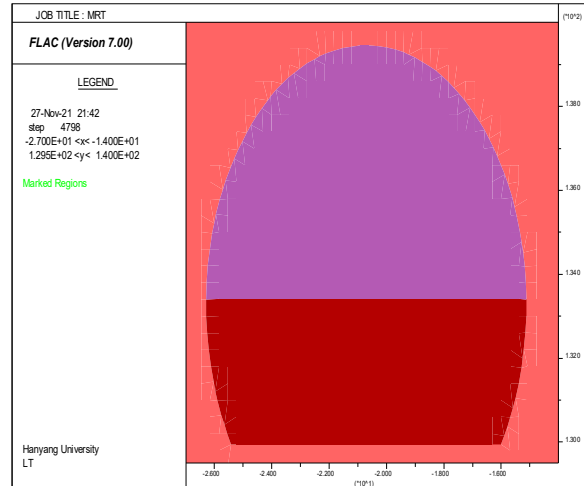
According to the Figure 4, all cases are stable. The maximum critical strain value is 0.065 for case 18, where the 20 MPa vertical stress acts on the SS2 rock mass of the KHP project. In this case, the stresses are high, and the rock mass strength is low

compared to other rock units in Table 3. The lowest value of the critical strain is 0.01 for case 4. This value corresponds to the highest rock mass strength in Table 3 and σ_v of 10 MPa, lower than 15 and 20 MPa. Comparing cases 1-6 (tunnel size = 7.12 m)

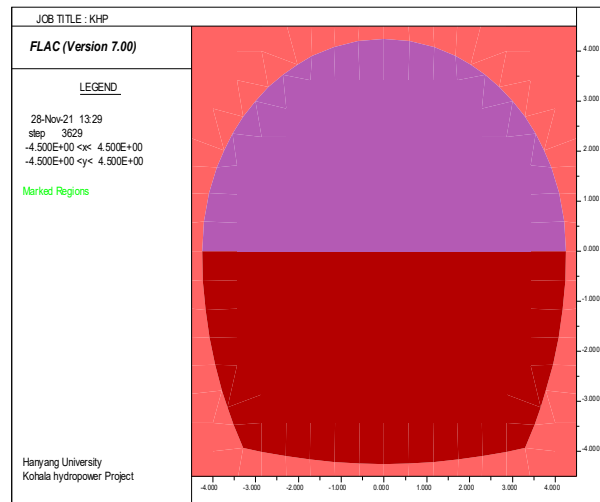
with cases 7-12 (tunnel size = 11.17 m), the results reveal that critical strain values increase with tunnel size, keeping the stresses and rock mass quality the same.



(a) Full face excavation of Lowari Rail Tunnel (case 1-6)



(b) Top heading and bench excavation sequence of Modified Road Tunnel (case 7-12)



(c) Top heading and bench excavation of the Headrace tunnel of Kohala hydropower project (case 13-18)

Figure 3. FLAC modelling, showing three excavation profiles and their sequence of excavation.

6.2. Evaluation based on stress reduction factor

Before tunnel excavation, the in-situ stress environment remains a function of principal stresses. During the excavation, redistribution of the stresses occurs due to which the virgin stress in the excavation vicinity changes. In the post-excavation scenario, the virgin stress field environment switches to induced principal stresses, the tangential (σ_θ) and radial stresses (σ_r), around the tunnel. These σ_θ and σ_r are at right angles but they are inclined to the direction of the virgin stress

field. In the induced stress environment, σ_r is the minimum principal stress that is negligible at the excavation periphery. This σ_r acts as confinement and increases with the distance from the tunnel periphery. On the other hand, σ_θ is the maximum principal stress, and is at its peak near the tunnel edge. This σ_θ gradually decreases with the distance from the tunnel boundary. The ratio of the σ_θ and σ_c is used as a stress level and a simple index for the tunnel stress-based stability [2].

The σ_{θ} was determined using the FLAC^{2D} and was used for the stress-strength ratio (σ_{θ}/σ_c) calculation. These ratios were plotted for different rock units, as shown in Figure. 5. These figures reveal that for the same rock unit and tunnel size, increasing the in-situ stresses results in an increased stress-strength ratio. For 10 MPa stress, the majority of the cases indicated stable conditions. In the case of $\sigma_v = 15$ MPa, most of the cases are in the tight structure zone, which according to Table 1, has no major issue. Only cases 3 and 9 showed moderate slabbing problems for $\sigma_v = 20$ MPa. Comparing the stress concentration around the tunnel periphery, derived from the excavation sequence adopted in this study with the actual excavation sequence of MRT revealed that the stress concentrations were higher in the top heading and bench excavation approach. The excavation sequence played a significant role as no such problems were observed during the MRT construction, although some audible brittle failure sounds were noticed during the construction of the LRT.

The stress-strength ratio values for the LRT cases were higher than MRT for the same stress and rock mass conditions. This inverse relation of the ratio with the tunnel size is due to a twice relaxation of rock mass during top heading and bench excavation of MRT, compared to the full-face excavation of LRT. During the excavation of MRT, the displacement is comparatively higher than LRT (Figure 4). This high displacement relaxed the rock mass and resulted in a comparatively low-stress concentration.

The magnitude of tangential stresses is not dependent on excavation size [4]. According to Kirsch Equation, these stresses are a function of the major and minor principal stresses only. Therefore, the stress-strength ratio values increase with increasing σ_v ; however, for the same magnitude of σ_v , the ratio decreases with rock strength, as shown in Figure 5. For the same tunnel size and σ_v magnitude, the ratios are comparatively lower for those rock units having the highest intact rock strength.

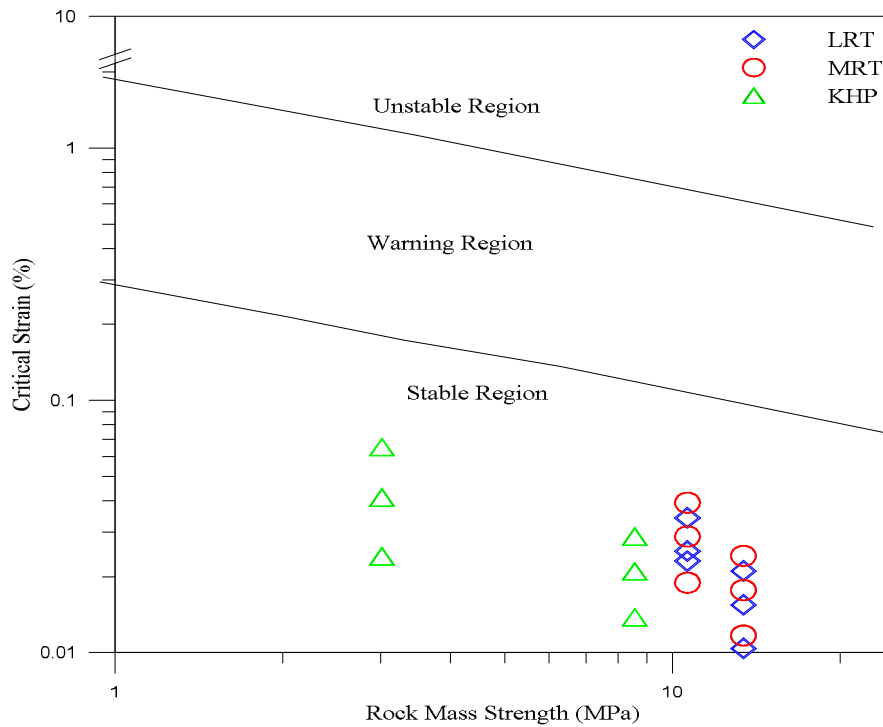


Figure 4. Strain-based tunnel evaluation of all cases of Table 2. For each rock mass quality/strength and tunnel size, critical strain increases with vertical stresses (10, 15, and 20 MPa).

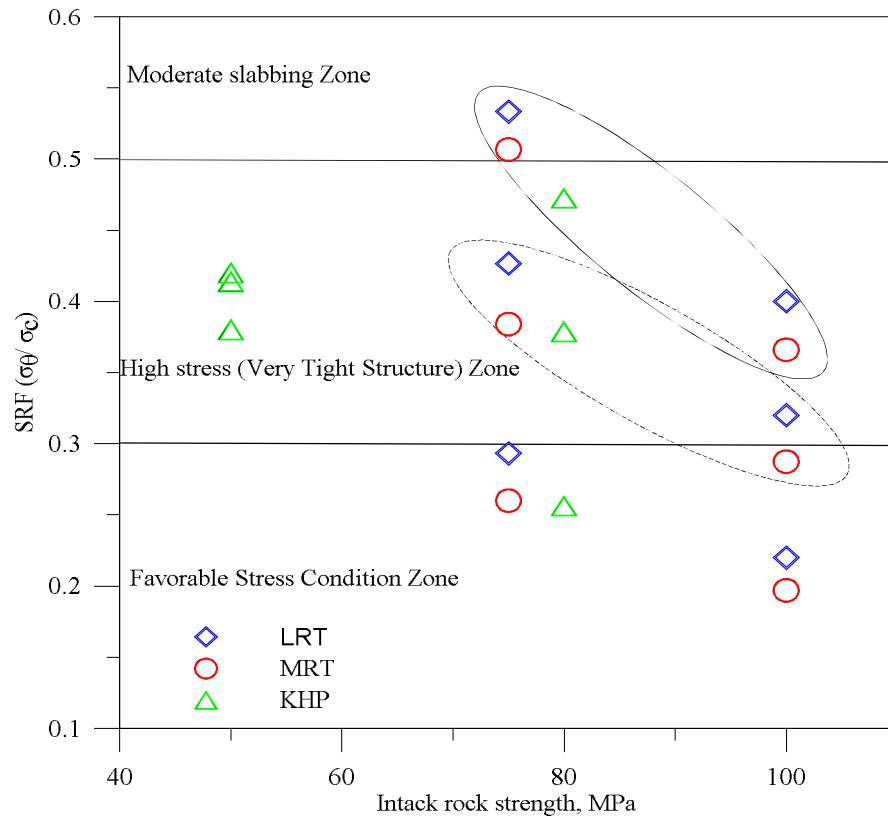


Figure 5. Stress-based tunnel stability evaluation of all cases of Table 2. The data in oval shapes full and dotted lines are 20 and 15 MPa vertical stress conditions, respectively. The remaining data are for 10 MPa cases.

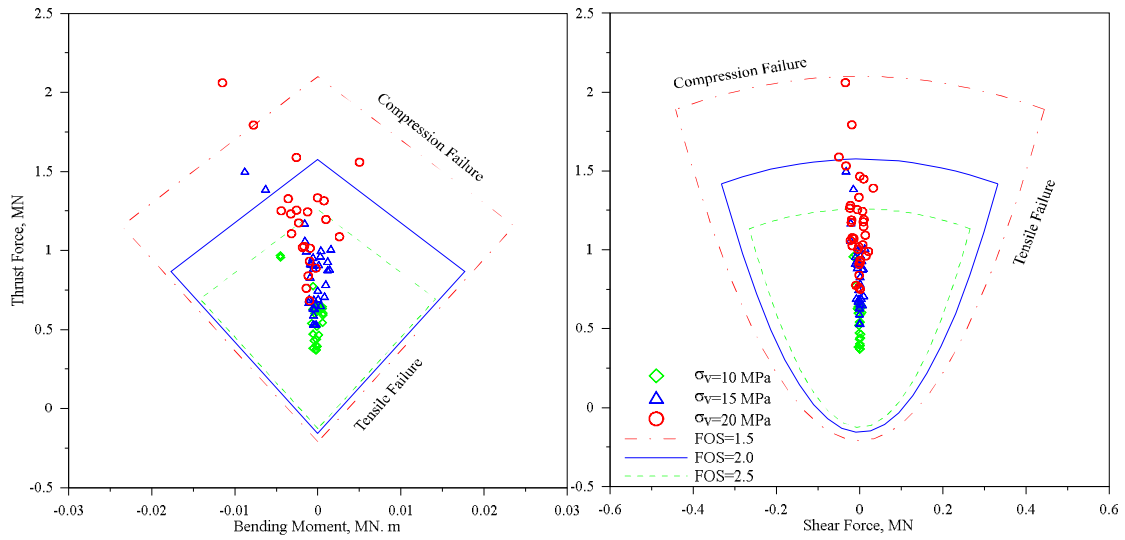
6.3. Stability evaluation based on capacity diagram

To get the developed thrust force, shear force, and bend moment in shotcrete, the structure liner axial fixscale option is used from the plot menu after solving the model statically. Equations 1-3 and 4-6 were used for the thrust-bending moments and thrust-shear forces diagram for FOS values equal to 1.5, 2, and 2.5. The shotcrete thickness values, listed in Table 4, were used as input to the numerical model. The simulated results are plotted in Fig. 6. The purpose was to quantify bending moment, thrust, and shear forces induced in the shotcrete. The utility function is used in the FLAC after solving the model statically for the liner information.

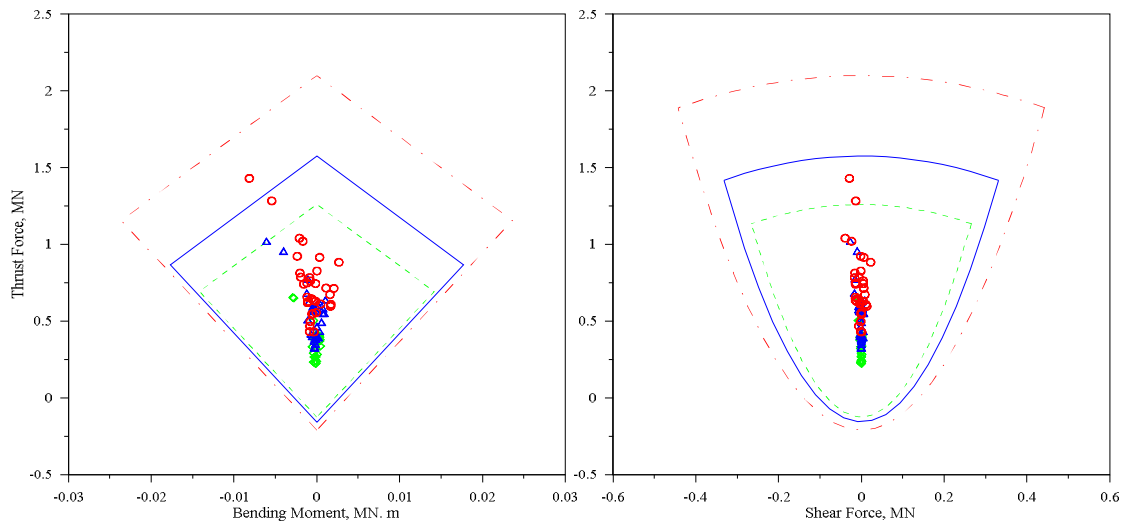
The results indicate that the applied liner/shotcrete in LRT is stable in compression and tension for both rock units of the project (granodiorite and gneiss) (Figures 6(a) and 6(b)). In the granodiorite rock unit, a low FOS in compression was observed for the highest stress level. Compared to the gneiss rock unit (Table 3), granodiorite rock mass has low strength and deformation modulus (E_{rm}). These low values show

high deformation and stress-strength ratio values for granodiorite than gneiss rock, as shown in Figures 4 and 5, respectively. Due to these high stresses and deformations, the liner experienced compression as the σ_v increased. In compression, low values of FOS with increasing σ_v were observed in all the cases, as shown in Figure 6.

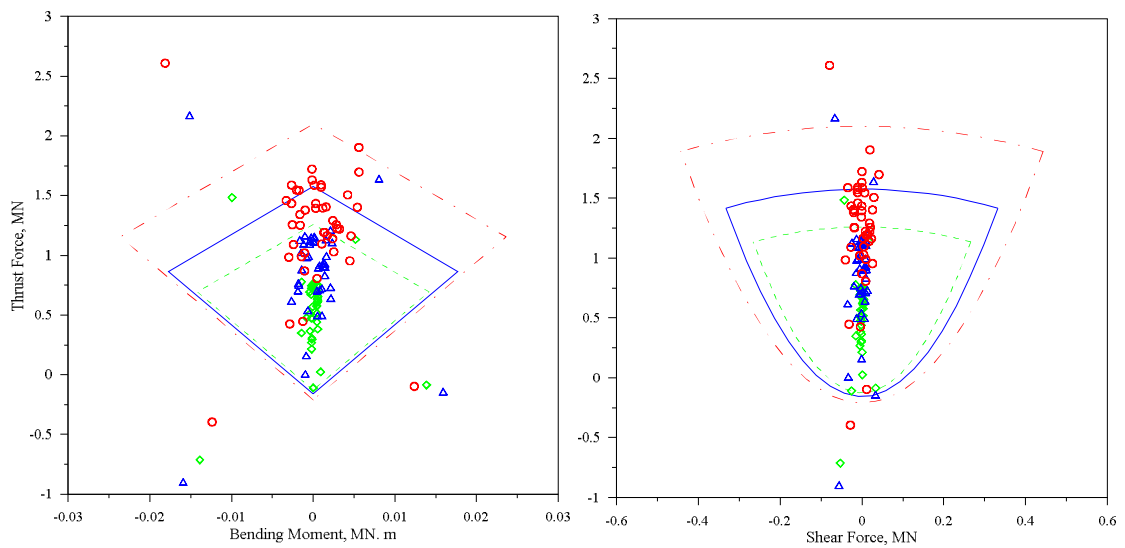
The remaining cases in Figure 6 (c-f) show liner instability in compression and tension. The shotcrete element with the stability issues in Figure 6, were determined and compared with numerical models. The shotcrete elements having instability issues were the corner elements in the top heading and bench excavation. These corners were the stress concentration zones. As the capacity diagram is based on the circular liner, the major principal stress contours were determined at these corners for cases 09 and 18 (where comparatively more elements show issues), as shown in Figure 7. This figure reveals a high concentration of major principal stress at the tunnel corners, both in the top heading and bench. As shown in Figure 4, the displacement is higher in case 18 (SS2 rock unit and $\sigma_v = 20$ MPa) than in case 09 (granodiorite rock unit and $\sigma_v = 20$ MPa); therefore, the stress concentration is higher in the latter case.



a). LRT (granodiorite)

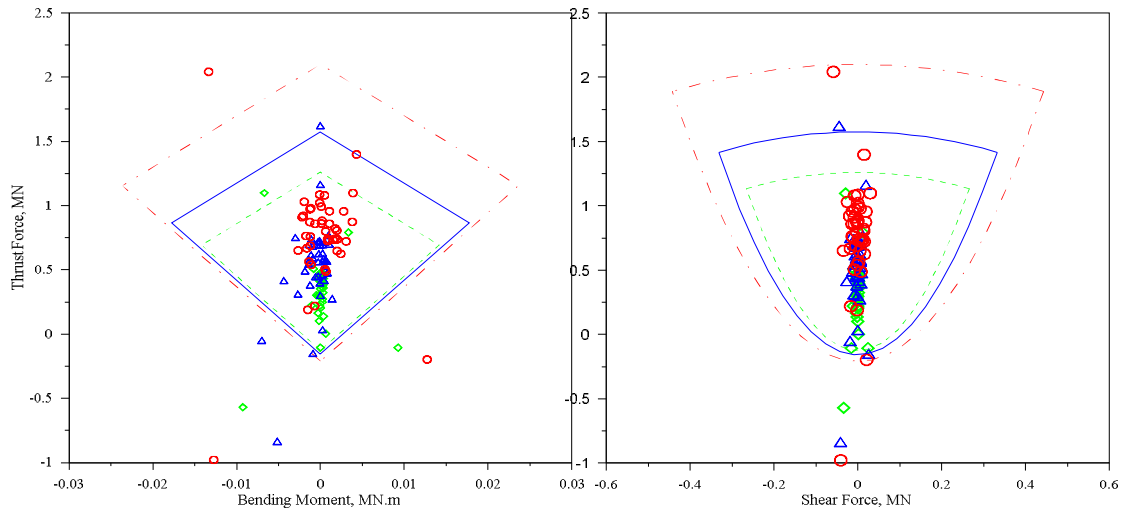


b). LRT (Gneiss)

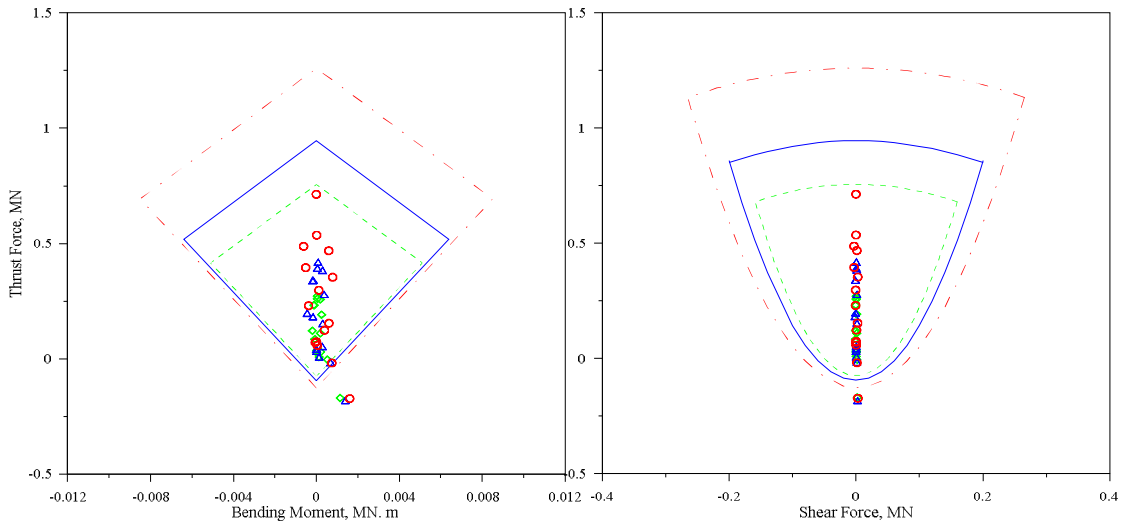


c). MRT (granodiorite)

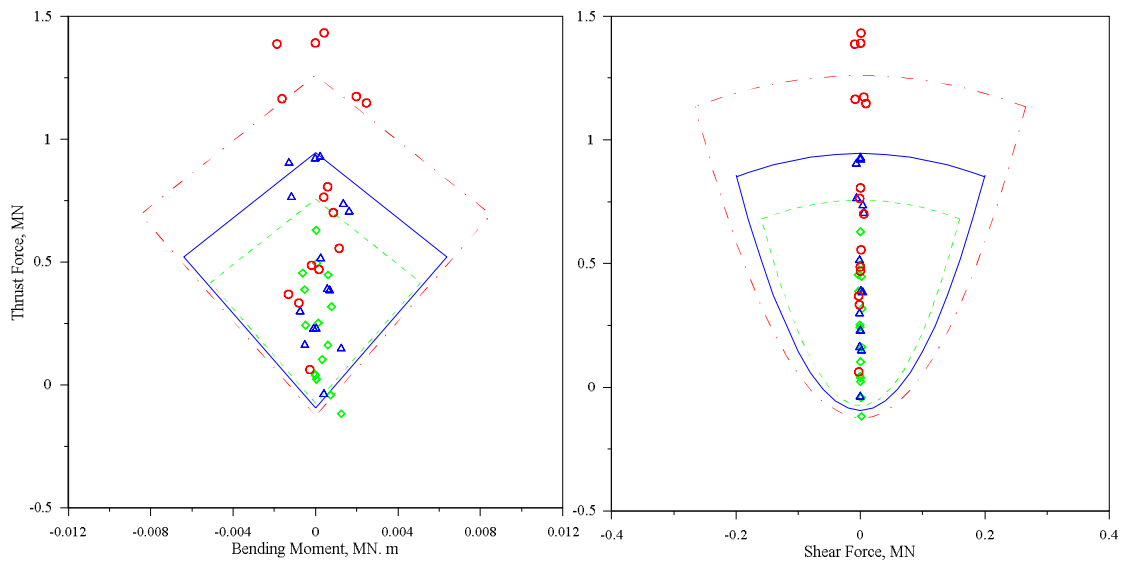
Figure 6. Shotcrete stability evaluation through capacity diagram.



d). MRT (Gneiss)

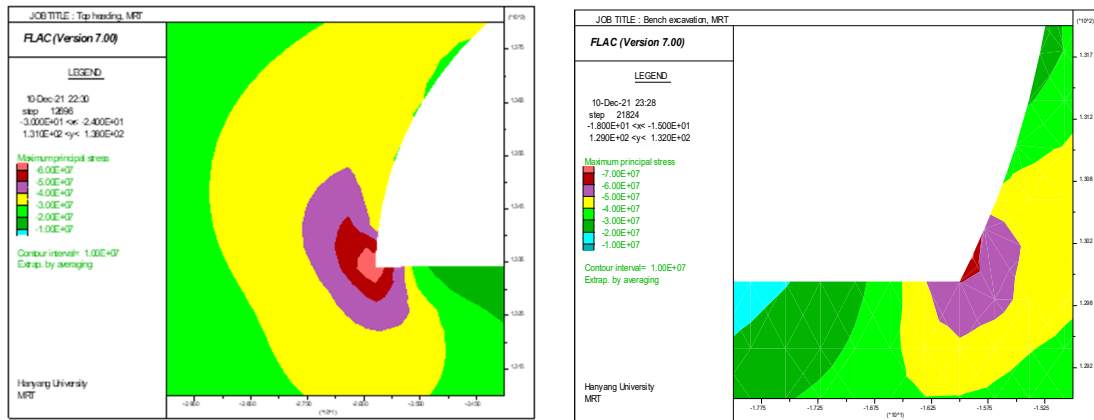


e). KHP (SS1)

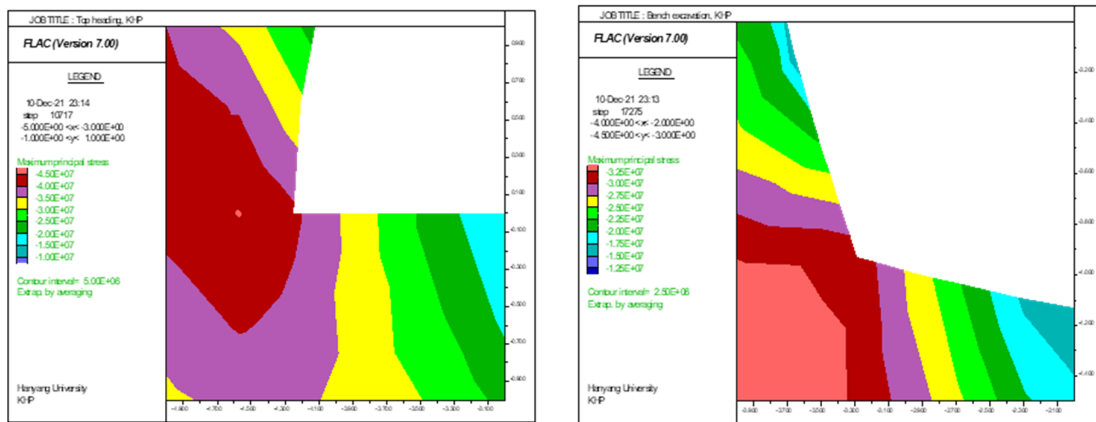


f). KHP (SS2)

Continous of Figure 6. Shotcrete stability evaluation through capacity diagram.



Case 09 (MRT, Granodiorite, $\sigma_v = 20$ MPa)



Case 18 (KHP, SS2, $\sigma_v = 20$ MPa)

Figure 7. Major principal stress state at corners (top heading (left) and bench (right)).

7. Conclusions

The following generalized conclusions were retrieved from this work:

- The tunnel does not seem to be stable if a stability trend occurs in one evaluation technique because each evaluation technique assesses the effect of individual parameters. Therefore, multiple evaluation techniques should be used for tunnel stability analysis.
- Tunnel behaviours are dependent on the rock mass mechanical properties, in-situ stresses, tunnel size, and the excavation sequence.
- The rock having high deformation modulus can cause stress concentration at the tunnel periphery. If the in-situ stresses are high, the excavation-induced tangential stresses can cause brittle failure and which can be evaluated using the SRF approach.
- In rock having low deformation modulus, the high tangential stresses can cause squeezing to occur, and in such cases, the instabilities can be evaluated using the critical strain approach.

- The stress concentrations in sharp corners of the tunnel cause instability issues in the liner and can be assessed from the capacity diagram. In such situations, using an appropriate tunnel shape can help overcome these instabilities.

Conflict of Interest

The authors declare that they have no conflict of interest.

References

[1]. Ali, W., Rehman, H., Abdullah, R., Xie, Q., and Ban, Y. (2022). Topography induced stress and its influence on tunnel excavation in hard rocks—a numerical approach. *GEOMATE Journal*. 22 (94): 93-101.

[2]. Barton, N. (2002). Some new Q-value correlations to assist in site characterisation and tunnel design. *International journal of rock mechanics and mining sciences*. 39 (2): 185-216.

[3]. Barton, N., Lien, R., and Lunde, J. (1974). Engineering classification of rock masses for the design of tunnel support. *Rock mechanics*. 6 (4): 189-236.

- [4]. Barton, N., Lien, R., and Lunde, J. (1974). Engineering classification of rock masses for the design of tunnel support. *Rock mechanics*. 6 (4): 189-236. doi:10.1007/bf01239496
- [5]. Bieniawski, Z.T. (1989). *Engineering rock mass classifications: a complete manual for engineers and geologists in mining, civil, and petroleum engineering*: John Wiley & Sons.
- [6]. Carranza-Torres, C., and Diederichs, M. (2009). Mechanical analysis of circular liners with particular reference to composite supports. For example, liners consisting of shotcrete and steel sets. *Tunnelling and Underground Space Technology*. 24 (5): 506-532.
- [7]. Daraei, A., and Zare, S. (2018). A new strain-based criterion for evaluating tunnel stability. *Geomechanics & engineering*. 16 (2): 205-215.
- [8]. Feng, X.T., and Hudson, J.A. (2011). *Rock engineering design*: CRC Press.
- [9]. Fu, J., Haeri, H., Yavari, M., Sarfarazi, V., and Marji, M. (2021). Effects of the Measured Noise on the Failure Mechanism of Pre-Cracked Concrete Specimens Under the Loading Modes I, II, III, and IV. *Strength of Materials*. 53 (6): 938-949.
- [10]. GEOCONSULT-TYPSA. (2004). *Geotechnical Interpretative Report, Lowari Tunnel*. Retrieved from
- [11]. Ghorbani, M., Shahriar, K., Sharifzadeh, M., and Masoudi, R. (2020). A critical review on the developments of rock support systems in high stress ground conditions. *International Journal of Mining Science and Technology*. 30 (5): 555-572.
- [12]. Grimstad, E., and Barton, N. (1993). Updating the Q-system for NMT. Paper presented at the Proc. int. symp. on sprayed concrete-modern use of wet mix sprayed concrete for underground support.
- [13]. Grimstad, E., and Barton, N. (1993). Updating the Q-system for NMT. Paper presented at the Proceedings of the International Symposium on Sprayed Concrete-Modern use of wet mix sprayed concrete for underground support, Fagemes, Oslo, Norwegian Concrete Association, 1993.
- [14]. Haeri, H. (2015). Simulating the crack propagation mechanism of pre-cracked concrete specimens under shear loading conditions. *Strength of Materials*. 47 (4): 618-632.
- [15]. Haeri, H., Sarfarazi, V., and Zhu, Z. (2017). Effect of normal load on the crack propagation from pre-existing joints using Particle Flow Code (PFC). *Computers and Concrete*. 19 (1): 99-110.
- [16]. Hoek, E. (1998). Tunnel support in weak rock. Paper presented at the Keynote address, Symposium of Sedimentary Rock Engineering, Taipei, Taiwan.
- [17]. Hoek, E. (2001). Big tunnels in bad rock. *Journal of Geotechnical and Geoenvironmental Engineering*. 127 (9): 726-740.
- [18]. Hoek, E., Carranza-Torres, C., and Corkum, B. (2002). Hoek-Brown failure criterion-2002 edition. *Proceedings of NARMS-Tac*, 1, 267-273.
- [19]. Hoek, E., and Marinos, P. (2000). Predicting tunnel squeezing problems in weak heterogeneous rock masses. *Tunnels and tunnelling international*. 32 (11): 45-51.
- [20]. Høien, A.H., Nilsen, B., and Olsson, R. (2019). Main aspects of deformation and rock support in Norwegian road tunnels. *Tunnelling and Underground Space Technology*, 86, 262-278.
- [21]. Hung, C. J., Monsees, J., Munfah, N., and Wisniewski, J. (2009). *Technical manual for design and construction of road tunnels—civil elements*. Retrieved from
- [22]. Khan, B., Jamil, S.M., Jafri, T.H., and Akhtar, K. (2019). Effects of different empirical tunnel design approaches on rock mass behaviour during tunnel widening. *Heliyon*. 5 (12): e02944.
- [23]. Kim, J.J., Lee, J.K., Kim, J.U., and Yoo, H.K. (2013). Evaluation of rock load based on critical shear strain concept on tunnels. *Journal of Korean Tunnelling and Underground Space Association*. 15 (6): 637-652.
- [24]. Lee, J.K., Yoo, H., Ban, H., and Park, W.-J. (2020). Estimation of rock load of multi-arch tunnel with cracks using stress variable method. *Applied Sciences*. 10 (9): 3285.
- [25]. Li, C.C. (2021). Principles and methods of rock support for rockburst control. *Journal of Rock Mechanics and Geotechnical Engineering*. 13 (1): 46-59.
- [26]. Lawson, A., and Bieniawski, Z. (2013). *Critical Assessment of RMR based Tunnel Design Practices: a Practical Engineer's Approach*.
- [27]. Mazaira, A., and Konicek, P. (2015). Intense rockburst impacts in deep underground construction and their prevention. *Canadian Geotechnical Journal*. 52 (10): 1426-1439.
- [28]. Munir, K. (2011). Development of correlation between rock classification system and modulus of deformation. UNIVERSITY OF ENGINEERING AND TECHNOLOGY LAHORE—PAKISTAN.
- [29]. Naji, A.M., Emad, M.Z., Rehman, H., and Yoo, H. (2019). Geological and geomechanical heterogeneity in deep hydropower tunnels: A rock burst failure case study. *Tunnelling and Underground Space Technology*, 84, 507-521.
- [30]. NGL (2015). Using The Q-system, Rock mass classification and support design. Retrieved from <https://www.ngi.no/eng/Services/Technical-expertise-A-Z/Engineering-geology-and-rock-mechanics/Q-system>
- [31]. Palmstrom, A., and Stille, H. (2007). Ground behaviour and rock engineering tools for underground excavations. *Tunnelling and Underground Space Technology*. 22 (4): 363-376.

- [32]. Panthi, K.K. (2012). Evaluation of rock bursting phenomena in a tunnel in the Himalayas. *Bulletin of Engineering Geology and the Environment*. 71 (4): 761-769.
- [33]. Park, S.H., and Shin, Y.S. (2007). A Study on the Safety Assessment Technique of a Tunnel Using Critical Strain Concept. *Journal of the Korean Geotechnical Society*. 23 (5): 29-41.
- [34]. Park, S., and Park, S. (2014). Case studies for tunnel stability based on the critical strains in the ground. *KSCE Journal of Civil Engineering*. 18 (3): 765-771.
- [35]. Rehman, H., Ali, W., Naji, A., Kim, J.-j., Abdullah, R., and Yoo, H.-k. (2018). Review of Rock-Mass Rating and Tunneling Quality Index Systems for Tunnel Design: Development, Refinement, Application and Limitation. *Applied Sciences*. 8 (8): 1250.
- [36]. Rehman, H., Ali, W., Shah, K.S., Mohd Hashim, M.H.B., Khan, N.M., Ali, M., and Junaid, M. (2022). The Finite Difference Analysis of Empirical Tunnel Support Design in High Stress fractured rock mass Environment at the Bunji Hydropower Project, Pakistan. *Journal of Mining and Environment*.
- [37]. Rehman, H., Naji, A., Kim, J.-j., and Yoo, H.K. (2018). Empirical Evaluation of Rock Mass Rating and Tunneling Quality Index System for Tunnel Support Design. *Applied Sciences*. 8 (5): 782.
- [38]. Rehman, H., Naji, A. M., Ali, W., Junaid, M., Abdullah, R. A., and Yoo, H.-k. (2020). Numerical evaluation of new Austrian tunneling method excavation sequences: A case study. *International Journal of Mining Science and Technology*.
- [39]. Rehman, H., Naji, A. M., Kim, J.-j., and Yoo, H. (2019). Extension of tunneling quality index and rock mass rating systems for tunnel support design through back calculations in highly stressed jointed rock mass: An empirical approach based on tunneling data from Himalaya. *Tunnelling and Underground Space Technology*, 85, 29-42.
- [40]. Rehman, H., Naji, A. M., Nam, K., Ahmad, S., Muhammad, K., and Yoo, H.-K. (2021). Impact of construction method and ground composition on headrace tunnel stability in the Neelum–Jhelum Hydroelectric Project: A case study review from Pakistan. *Applied Sciences*. 11 (4): 1655.
- [41]. Sakurai, S. (1997). Lessons learned from field measurements in tunnelling. *Tunnelling and Underground Space Technology*. 12 (4): 453-460.
- [42]. Sarfarazi, V., Haeri, H., Shemirani, A. B., and Zhu, Z. (2017). Shear behavior of non-persistent joint under high normal load. *Strength of Materials*. 49 (2): 320-334.
- [43]. Schubert, W., and Goricki, A. (2003). The guideline for the geomechanical design of underground structures with conventional excavation.
- [44]. Society, B.T. (2004). *Tunnel lining design guide*: Thomas Telford.
- [45]. Stille, H., and Palmström, A. (2008). Ground behaviour and rock mass composition in underground excavations. *Tunnelling and Underground Space Technology*. 23 (1): 46-64.
- [46]. Wang, C., and Bao, L. (2014). Predictive analysis of stress regime and possible squeezing deformation for super-long water conveyance tunnels in Pakistan. *International Journal of Mining Science and Technology*. 24 (6): 825-831.
- [47]. Wu, K., Shao, Z., Qin, S., Wei, W., and Chu, Z. (2021). A critical review on the performance of yielding supports in squeezing tunnels. *Tunnelling and Underground Space Technology*, 115, 103815.
- [48]. Yang, J., Wang, S., Wang, Y., and Li, C. (2015). Analysis of arching mechanism and evolution characteristics of tunnel pressure arch. *Jordan Journal of Civil Engineering*. 9 (1).
- [49]. Yim, S., Seo, Y., Kim, C., and Kim, K. (2011). Critical strain concept-based simple method for pre-evaluation of tunnel face safety using RMR. *Procedia engineering*, 14, 3147-3150.
- [50]. Zhang, C., Feng, X.-T., Zhou, H., Qiu, S., and Wu, W. (2012). Case histories of four extremely intense rockbursts in deep tunnels. *Rock mechanics and rock engineering*. 45 (3): 275-288.

بررسی اثر اندازه تونل، شرایط توده سنگ و تنش‌های برجا بر پایداری تونل‌ها

حافظ الرحمن^{۱،۲}، احمدشاه^۱، محدحزیزان بن محد هاشم^{۳*}، ناصر محمد خان^۱، وحید علی^۱، کوثر سلطان شاه^۲، محمد جنید^۲، رفیع الله^{۴،۵}، و محمد بلال عادل^۶

۱. گروه مهندسی معدن، دانشکده فنی، دانشگاه فناوری اطلاعات بلوچستان، علوم مهندسی و مدیریت (BUITEMS)، کوئته، پاکستان
۲. دانشکده مهندسی مواد و منابع معدنی، دانشگاه ساینز مالزی، پردیس مهندسی، نیبونگ تبال، پنانگ، مالزی
۳. گروه مهندسی معدن، دانشگاه بین المللی قراقرام، گیلگیت-بالتستان، پاکستان
۴. گروه ژئوتکنیک و حمل و نقل، دانشکده مهندسی عمران، دانشگاه تکنولوژی مالزی، جوهر بحرو، جوهر، مالزی
۵. گروه مهندسی زمین شناسی، دانشکده فنی، دانشگاه فناوری اطلاعات بلوچستان، علوم مهندسی و مدیریت (BUITEMS)، کوئته، پاکستان
۶. گروه حمل و نقل و مهندسی ژئوتکنیک، دانشگاه ملی علم و صنعت، پردیس ریسالپور، پاکستان

ارسال ۲۰۲۲/۰۹/۲۴، پذیرش ۲۰۲۲/۱۱/۰۹

* نویسنده مسئول مکاتبات: mohd_hazizan@usm.my

چکیده:

عوامل اصلی مؤثر بر پایداری تونل شامل شرایط زمین، تنش‌های برجا و ویژگی‌های مرتبط با پروژه است. در این کار تحقیقاتی از کرنش بحرانی، ضریب کاهش تنش (SRF) و نمودارهای ظرفیت برای تحلیل پایداری تونل استفاده شده است. برای این منظور هجده مقطع تونل با استفاده از نرم افزار FLAC2D مدل سازی شده است. خواص توده سنگ برای مدل سازی با استفاده از نرم افزار RocLab به دست آمده است. نتایج به دست آمده نشان می‌دهد که تغییر شکل‌های تونل در اکثر موارد در حد ایمنی است. در همین حال، مشاهده می‌شود که کیفیت توده سنگ، اندازه تونل و تنش‌های برجا به تغییر شکل کمک می‌کنند. تغییر شکل‌های حاصل بر SRF نیز تاثیر می‌گذارد. SRF به تنش‌های درجا، کیفیت توده سنگ و توالی حفاری بستگی دارد. نمودارهای ظرفیت نشان می‌دهد که لاینر شکست‌های ناشی از استرس را به دلیل تمرکز تنش در گوشه‌های تونل تجربه می‌کند. این مطالعه نتیجه می‌گیرد که تحلیل پایداری تونل باید شامل یک رویکرد یکپارچه باشد که کیفیت سنگ، تنش درجا، ابعاد حفاری و تغییر شکل‌ها را در نظر می‌گیرد.

کلمات کلیدی: کرنش بحرانی، ضریب کاهش تنش، نمودار ظرفیت، شکل و اندازه تونل، تنش‌های برجا.